Targeted Disruption of PDCD2 Delays G1/S Transition in Lung Carcinoma by Inhibiting Cyclin D1 Transcription

Nora Barboza[1,*], Daniel J. Medina[1*], Garima Sinha[2], Evita Sadimin[1], Kuo-Chieh Lee[1], Gulam M. Rather[1] and Steven J. Greco[2]

[1]*Rutgers, Robert Wood Johnson Medical School, Rutgers and Cancer Institute of New Jersey, 195 Little Albany Street, New Brunswick, NJ 08901, United States*
[2]*Department of Medicine-Hematology/Oncology. Rutgers-New Jersey Medical School, MSB, E-579 185 South Orange Avenue. Newark, NJ 07103, United States*
E-mail: medinadj@comcast.net; barbozanora@gmail.com
[*]*Corresponding Authors*

Received 01 June 2023; Accepted 28 September 2023;
Publication 03 February 2024

Abstract

We previously reported on high expression of define PDCD2 in human malignancies. Knockdown of PDCD2 reduced the proliferation of leukemia and lung carcinoma cells. However, the mechanism by which PDCD2 reduces tumor proliferation remains unclear. This study tested the hypothesis that lowered PDCD2 would delay the proliferation of A549 lung carcinoma cells. Entry of A549 cells into S-phase was significantly (p-value 0.05) delayed when PDCD2 was knockdown. This correlated with a significant downregulation of cyclin D1, and AKT phosphorylation. Inhibition of the PI3K/AKT signaling pathway by Ly294002 decreased levels of PDCD2. These findings are consistent with a role for PDCD2 to mediate the entry of A549 cells into the cell cycle. Resting A549 cells showed PDCD2 localizing in the nucleus and plasma membrane and became diffuse with cell division, suggesting that PDCD2 is mitogen-dependent and may be involved in the proper timing

International Journal of Translational Science, Vol. 1, 53–76.
doi: 10.13052/ijts2246-8765.2024.004
© 2024 River Publishers

of cell cycle. These findings may represent a promising venue to develop PDCD2 in clinical applications.

Keywords: Cell Proliferation, Cell Cycle Delayed, Cyclin D1, S Phase, Quiescent, Ubiquitous, Mitogen, Lung cancer, PI3K/AKT.

Introduction

The protein Programmed Cell Death 2 (PDCD2) was isolated as a cDNA of death-associated mRNAs from a subtractive library of untreated and dexamethasone-treated thymocytes [1]. The assignment of *PDCD2* as a death-associated gene was based on its enforced expression to cause a modest increase in apoptosis, which was attenuated by the caspase 3 inhibitor z-DEVD-fmk, and the pan-caspase inhibitor z-VAD-fmk [2, 3]. This implicated the caspase pro-apoptotic machinery to partly explain the mechanism of PDCD2-mediated cell death. However, other studies, including models of Drosophila, failed to corroborate PDCD2 as proapoptotic [4–7]. PDCD2 has been identified as a target of the transcriptional repressor BCL6 [2, 3, 8] and as a tumor suppressor due its decreased expression in cancer cells [9].

PDCD2 is linked to the development and self-renewal of embryonic stem cells, as the inner cell masses of *Pdcd2*$^{-/-}$ blastocysts failed to show outgrowth [10]. PDCD2 has been implicated in hematopoiesis [11–13]. In other studies, PDCD2 decrease induced p53 and cell cycle arrest, indicating that PDCD2 could be a transcriptional regulator and cell cycle control [14].

PDCD2 interacts with N-CoR/mSin3A histone deacetylase (HDAC) to repress complexes and host cell factor 1 (HCF-1) [15]. HCF-1 activates various stages of the cell cycle and interacts with E2F proteins to regulate cell cycle-specific transcription [16–18]. PDCD2 MYND domain, a homologue of ETO/MTG8 MYND domain, can bind to N-CoR, associated to HDAC, to repress transcription [15, 19, 20]. Although the above studies in divergent models suggest a role for PDCD2 in the regulation of cell proliferation and differentiation, the biological function of PDCD2 remains an area of investigation.

We reported on timeline *PDCD2* expression in clinical isolates obtained from patients with hematologic malignancies [21]. Elevated expression at diagnosis was followed by a dramatic decrease in patients who responded to therapy, supporting a role for PDCD2 in treatment response. The findings were further analyzed in two cancer cell lines, A549 non-small cell lung cancer (NSCLC) and Jurkat T lymphoma cells. The results showed a decrease

in cell proliferation when PDCD2 was knockdown (KD) with no change in cell viability. Altogether, these observations support the involvement of PDCD2 in cell cycle progression.

Here we report on the mechanisms involved in the previously described delay in A549-PDCD2 KD cell proliferation. The results suggested that PDCD2 could regulate cyclin D1 expression. We provide mechanistic insights into how PDCD2 could alter cell cycle of A549 cells. The findings are discussed in the context of PDCD2 to interact with N-CoR/mSin3A histone deacetylase and/or HCF-1 to regulate cyclin D1 [15, 19, 20].

Materials and Methods

Reagents

The following were obtained from Millipore Sigma (St Louis, MO): Dulbecco's modified Eagle's (DMEM)/F-12 medium. fetal bovine serum (FBS), glutamine and penicillin-streptomycin 100 U/mL, dimethylsulfoxide (DMSO), API-2 (124012 – 10 mM stock solution). rapamycin (R0395 – 2 mM stock solution), and LY294002 (L9908 – 20 mM stock solution); U0126 (V1121 10 mM stock solution) from Promega (Madison, WI); G418 (11811-031 50 mg/ml stock solution) and lipofectamin 3000 from Invitrogen (Carlsbad, CA). The drugs were dissolved in DMSO and stock solutions were stored at 4°C. The following were obtained from ThermoFisher Scientific (Walthan, MA): DAPI, LY294002 (PI3K inhibitor, 5 uM), PKC inhibitor (5 μM), Velcade (NFkB inhibitor – 10 nM, 25 nM, 50 nM), Alexa Fluor® 647, propidium iodide, and SuperSignal West Femto Maximum Sensitivity Substrate.

Antibodies

Polyclonal antibody against PDCD2 was obtained from the Sharp Laboratory [15], mouse monoclonal Rb (G3-245) from BD Biosciences, Cdc2 (CDK1, H-17), CDK2 (6248), CDK4 (H-22), CDK6 (C21), anti-cyclin A (239), -cyclin D1 (H295), -cyclin E (247), -Thymidine Kinase, -E2F1, -E2F2 and -β-actin were from Santa Cruz Biotechnology (Santa Cruz, CA); rabbit monoclonal Akt PAN (C67E7), rabbit phospho-Akt Thr308 (D25E6), rabbit phospho-Akt Ser473 (D9E), rabbit monoclonal phospho-GSK-3β Ser9 (5B3), mouse-Rb (4H1), rabbit phospho-Rb Ser780 (D59B7), rabbit phospho-Rb Ser795, rabbit phospho-Rb Ser807/811 (D20B12), rabbit-c-Raf

(D4B3J), phospho-c-Raf Ser259, and Glyceraldehyde-3-phosphate dehydrogenase (GAPDH) HRP conjugate antibodies from Cell Signaling (Danvers, MA); rabbit GSK3β (AP8121a) antibody from Abgent from Woburn, MA; mouse-E2F1 (KH20 & KH95) antibody from Millipore Sigma (Burlington, MA); goat anti-mouse F(ab')2 fragment (Jackson ImmunoResearch, West Grove, PA); γ–tubulin was from Abcam (Waltham, MA), rabbit gamma-Tubulin from Bethyl Laboratories, Inc (Montgomery, Tx); mouse monoclonal Ki67 (NCL-Ki67-MM1) from Novocastra (Deer Park, IL); Alexa Fluor 488 goat anti-rabbit IgG (A-11034) and Alexa Fluor 594 donkey anti-mouse IgG (A-21203) from Invitrogen.

Cell Lines

A549 non-small cell lung cancer cell line was obtained from the American Type Culture Collection (Manassas, VA) and maintained in DMEM)/F-12 supplemented with 10% heat inactivated FBS. 2 mM glutamine, and 100/ml penicillin and streptomycin. A549 PDCD2 KD cells and the resistant A549 PDCD2 knockdown siRNA with functional expression vector (A549-PDCD2 expression) were previously described [21]. A549-PDCD2 contained a mutated site that prevents binding to the siRNA [21]. We maintained the engineered cells as for the parental A549, except with G418 (400 μg/ml).

Vectors

pGL3- cyclin D1 with the 5′ regulatory cyclin D1 upstream sequence (-1/-1748) was obtained from Addgene (Cambridge, MA); pGL3 basic, pGL3 control and pβgal were purchased from Promega (Madison, WI).

Transfection and Reporter Assay

The methods for transfection and reporter gene assay were previously described [22]. Briefly, cells were transiently transfected with Lipofectamin 3000. Co-transfection with pβgal served to normalize the transfection. Cells (3×10^5/well in a six well plates) were incubated in DMEM/F-12 with 2% FBS, 2 mM glutamine, penicillin 100 U/mL, streptomycin 100 U/mL and 1X transferrin (Invitrogen). After 4 h, A549 WT, PDCD2-A549 and PDCD2 shRNA A549 were transfected with pGL3-cyclin D1 in the presence of the following pharmacological inhibitors: LY294002 (PI3K inhibitor, 5 μM), PKC (5 μM) or Velcade (NFκB inhibitor at 10, 25 or 50 nM). Control wells contained vehicle (DMSO). After 16 h, whole cell lysates were quantified for luciferase and β-galactosidase activity.

Lysates were prepared as follows: Adherent cells were washed with PBS (pH 7.4) and then scraped in PBS. The cells were pelleted, first by lysing with 1X reporter lysis buffer (Promega) followed by five cycles of freeze-thaw in dry ice/ethanol. After this, we removed the cell debris by centrifugation. The soluble fraction was quantified for total protein using Bio-Rad protein assay (Bio-Rad, CA) followed by quantification for luciferase and β-gal activities with the Luciferase Assay and β-galactosidase Enzyme Assay kits (Promega), respectively. The values for βgal activity were used to normalize luciferase activity. The data are presented as fold changes over empty vector. Positive control used pGL3 basic and negative control, empty pGL3.

Cell Cycle Analysis

EdU (5-ethynyl-2′- deoxyuridine) (Invitrogen) incorporation was used to analyze G1/S progression. Serum starved cells were seeded in triplicate at 0.5×10^6 cells per 10 cm plate in media with 0.1% FBS. After 72 h, the cells were stimulated with media containing 10% FBS. Cells were pulsed for 30 min with EdU (10 μM) and then harvested at different time points. The harvested cells were co-labeled with Alexa Fluor® 647 and propidium iodide according to the manufacturer's protocols. Proliferation was based on newly synthesized DNA to calculate the percentage of Alexa Fluor® 647 stained cells using the Cell Quest software. A minimum of 10,000 cells per sample was analyzed. Cell cycle analysis with propidium iodide staining was performed using standard methodologies [Propidium Iodide (PI) RNase staining buffer, BD Pharmingen]. Fluorescent intensities were acquired on a BD FACS Calibur™ and the percentage of cells in each phase of the cell cycle was calculated using the ModFit v3.0 software (BD Biosciences).

Western Blot

The method for western blot was previously described [21]. Briefly, denatured cell lysates were electrophoresed on gradient 4–12% polyacrylamide gels followed by transfer to polyvinylidene difluoride membranes (Perkin Elmer, Boston, MA). Membranes were blocked with 0.25% dry milk dissolved in 1X TBS plus 0.1% tween, and then probed with the respective antibodies followed by incubation with peroxidase-conjugated secondary antibody. The secondary antibodies were detected with chemiluminescence using SuperSignal West Femto Maximum Sensitivity Substrate. Band densities were normalized to the housekeeping genes with UN-SCAN-IT densitometry software (RRID:SCR_017291; Silk Scientific; Orem, UT).

Quantitative Real-time RT-PCR Analysis

Real-time PCR was performed as described [23]. Total RNA was isolated from cells using RNeasy Mini Kit (QIAGEN), according to the manufacturer's instructions. RNA was quantified with QIAxpert and then converted to cDNA with the High-Capacity cDNA Reverse Transcription Kit. Real-time PCR used the AgPath-ID One-Step RT-PCR Kit (Ambion/Applied Biosystems, Austin, TX) and the 7300 Real-Time PCR System (Thermo Fisher Scientific). Each sample was tested in technical and biological replications. The levels of test samples were normalized to β-actin levels. The reactions used the following primers: β-actin – Forward 5′-GTC TTC CCC TCC ATC GTG-3′; Reverse 5′-CAT GTC GTC CCA GTT GGT G-3′; and probe (5′6-FAM) CAT CCT CAC CCT GAA GTA CC-(3′ Iowa Black®FQ) (Integrated DNA Technologies, Coralville, IA); PDCD2 – Forward 5′-GCT GCA TCT TCC TCT TCT GC-3′; Reverse 5′-GGG GAG GGA TTC TCA GAA GGT-3′; and probe (5′-6-FAM) CCT GCG AGT TTT TAG GAA TCA (3′ Iowa Black® FQ) (Integrated DNA Technologies); Cyclin D1 (Hs00765553) primers from Applied Biosystems.

Immunostaining

A549 cells were plated on a cover-glass in a 12-well plate, and then cultured in DMEM/F-12 media plus 0.1% FBS. After 72 h, cells were fixed or stimulated with media plus 10% FBS for 22 h. Cells were fixed with 4% formalin (diluted in PBS) for 30 mins at RT and washed 3 times in PBS/Glycine. Antibody staining was processed as previously described [24]. Briefly, cells were incubated in primary block (130 mM NaCl, 7 mM Na_2HPO_4, 3.5 mM NaH_2PO_4, 7.7 mM NaN_3, 0.1% BSA, 0.2% Triton X-100, 0.05% Tween-20) +10% goat serum for 45–60 mins at RT, followed by a secondary block [IF Buffer + 10% goat serum + 20 μg/ml of goat anti-mouse F(ab′)2 fragment for 30-40 mins. Primary antibody staining was done overnight at 4° C, followed by three washes with IF buffer at RT and probed with secondary antibody for 60 mins at RT. Mouse monoclonal γ–tubulin, rabbit gamma-Tubulin (A302-631A), and mouse monoclonal Ki67. Antibodies were used at 1:100 dilution. The secondary antibodies were Alexa Fluor 488 goat anti-rabbit IgG (A-11034) and Alexa Fluor 594 donkey anti-mouse IgG (A-21203), used at 1:200 dilution. Nuclei were counterstained with 0.5 ng/ml DAPI. Samples were mounted in Prolong Gold anti-fade (Invitrogen, P36934) followed by capturing of the images were captured with a Zeiss Axiovert inverted fluorescent microscope.

Tissue Array Immunohistochemistry

A lung tissue microarray slide containing 200 cores of normal lung and lung carcinoma was obtained from US Biomax, Incorporated (Rockville, MD. The slide was stained with PDCD2 antibody at 1/1000 (was this directly conjugated and if so what?). The localization and intensity of the staining were evaluated blindly by a pathologist and the results were evaluated by a biostatistician.

Statistical Analyses

Statistical analyses were performed using the two tailed Student's t-test. A p value less than 0.05 was considered to be statistically significant.

Results

Delayed Cell Cycle Progression of PDCD2 Knockdown A549 Cells

We previously reported on reduced cell proliferation in PDCD2 KD lung cancer cells [21]. Since reduced cell proliferation could not be explained by cell senescence or cell death, we proposed that PDCD2 may regulate cell cycle. Henceforth, we used PDCD2 KD A549 lung cancer cells to dissect the role of PDCD2 in cell cycle regulation.

A549 PDCD2 KD cells were synchronized at the G0 phase by incubating the cells in media with 0.1% FBS. After 72 h, the cells were induced to cycling by changing the media with fresh media containing 10% FBS. At different times, the cells were analyzed for cycling phase by assessing the DNA content. Untransfected and empty vector (EV) transfected A549 cells showed S phase transition by 15 h (Figure 1A). In contrast, A549 PDCD2 KD cells showed a delay to S Phase at 24 h (Figure 1A).

Next, we performed time course studies on the cycling progression of wild type and KD A549 PDCD2 cells. We initiated the studies when the media were changed to contain 10% FCS. The cells were double labeled with Alexa Fluor 647 and propidium iodide and then analyzed by flow cytometry for cell cycle phase (Figures 1B, 1C and Supplemental Figure 1). The results showed A549 WT cells transitioning from S phase to G2 phase at 21 h, indicating a doubling time of 22.3 h [25] (Figure 1B). The cells completed full cycle by 48 h (Figures 1B and 1C). In contrast, PDCD2 KD cells were in S phase between 24 and 32 h (Figure 1B). A summary of the S phase

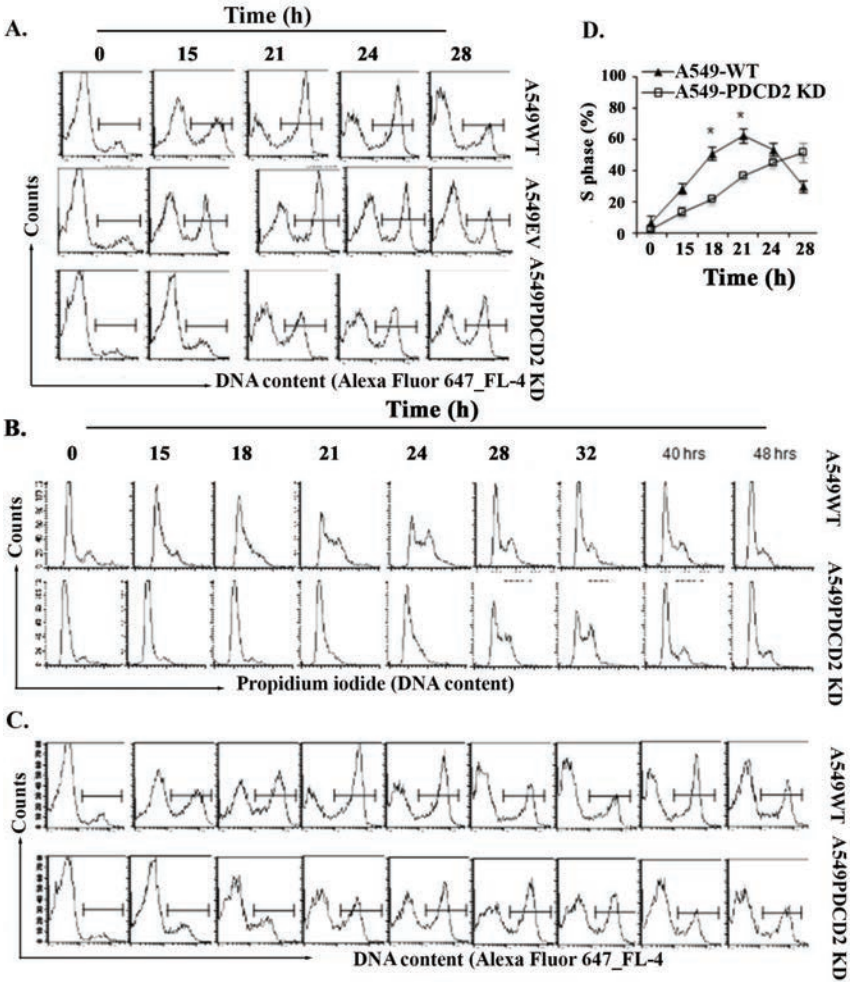

Figure 1 Delayed entry into the S phase of A549-PDCD2 KD after serum stimulation. After 72 hrs, of serum starvation cells were stimulated with medium containing 10% FBS and were cultured for the indicated time points. (A) Cell proliferation analysis of A549 PDCD2 KD compared to controls A549 wild type (WT) and A549 empty vector (EV). DNA synthesis, as a correlate of S phase transition by staining with Alexa Flour® 647 and propidium iodide. (B) Acquisition of propidium iodide stained cells was detected with FL-2, and cell proliferation (C) was determined by EdU incorporation detected with Alexa Flour® 647 (FL-4). The percentage of cells in S phase from each time point was calculated and plotted according to the flow cytometric analysis (D). The results presented represent the mean and standard deviations of at least three independent experiments.

results showed a significant delay of cell cycle by PDCD2 KD A549 cells, as compared to WT A549 cells (Figure 1D). These results indicated that PDCD2 KD significantly delayed but did not prevent G0-S transition of A549 cells.

Increased Ki-67 in PDCD2 Expressing A549 Cells

The studies in Figure 1 showed a role for PDCD2 in the proliferation of A549 cells. We further investigated this finding by performing immunocytochemistry for Ki-67. Time 0 used fixed A549 WT cells at the end of serum starvation as for Figure 1 (72 h in 0.1% FBS). After changing the media with 10% FBS, the cells were fixed at different time points. Fixed cells were double-labeled for PDCD2 and γ–tubulin, or PDCD2 and Ki-67 (Figure 2).

At time 0 (0 h, unstimulated), PDCD2 was localized to the nuclei and partially at the cell membrane and γ–tubulin in the cytoplasm, and 25% positive for nuclear Ki67 (Figures 2A and 2B). Upon stimulation with serum, PDCD2 was detected throughout the cells (Figure 2C). At 24 h, PDCD2 colocalized with γ–tubulin, and Ki-67 was increased by 60% (Figures 2D and 2E). Since γ-tubulin and Ki67 are prototypical markers of proliferation at the beginning of mitosis [26–28], we deduced that these findings confirmed a pivotal role for PDCD2 in cell cycle progression.

Decreased Cyclin D1 in PDCD2 Knockdown A549 Cells

In order to understand the molecular mechanism of delayed cell cycle by the A549 PDCD2 KD cells, we assessed cell cycle protein with extracts from KD with WT cells by western blots. We analyzed CDK1, CDK2, CDK4, CDK6, cyclin A, cyclin D, and cyclin E proteins. Extracts were collected from cells that were serum starved as described for Figure 1, from cells that were induced into cycling with media containing 10% FCS. We selected the 15 h time point to initiate the analyses because the cells were shown to be in late G1 phase at this time point (Figure 1A).

Cyclin quiescent PDCD2 KD cells showed lighter bands for cyclin D1, as compared to wild type cells (Figure 3A and Supplemental Figure 2). Similarly, there were minimal changes in the CDKs between the knockdown and wild-type A549 cells (Figure 3A, Supplemental Figure 2). We asked if decreased cyclin D1 was reflected at the transcript by real time PCR. This was assessed with cells placed in 10% FCS, at daily intervals up to 96 h. Real-time PCR verified PDCD2 KD at each time point (Supplemental Figure 3). Cyclin D1 mRNA levels remained constant in WT

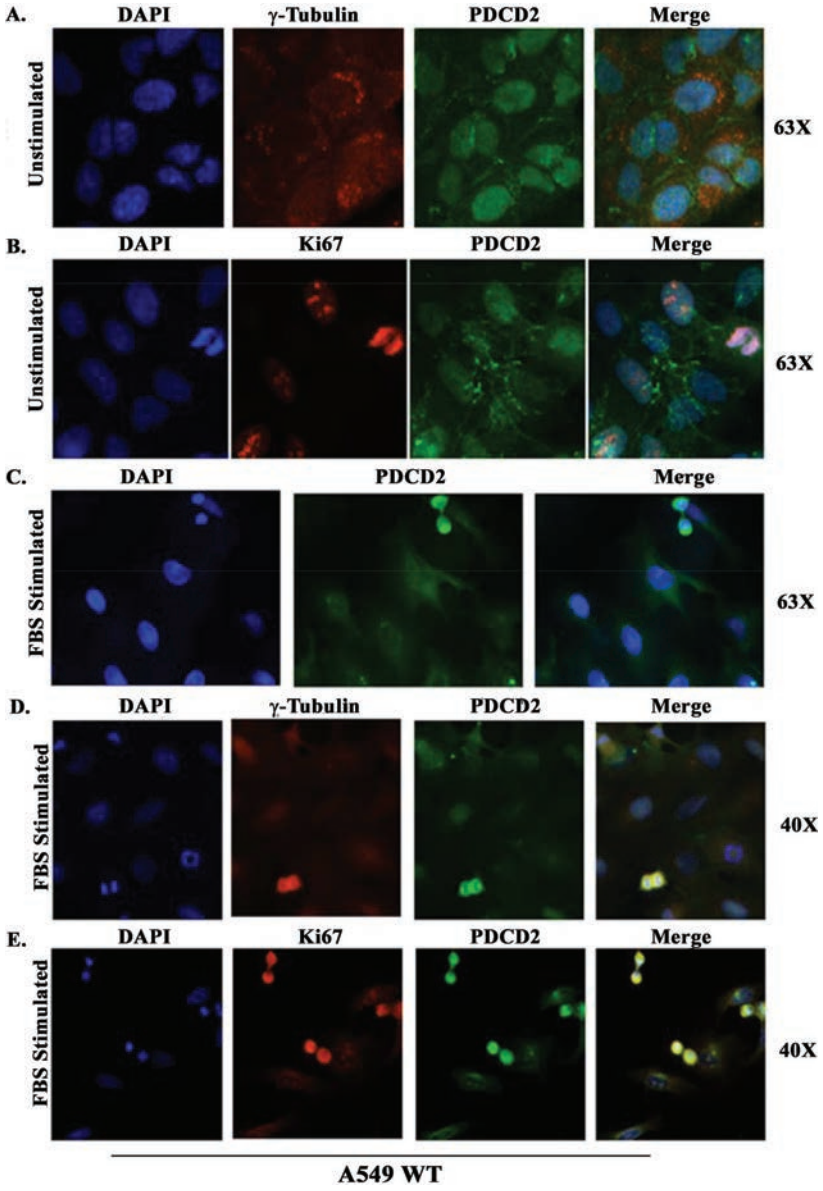

Figure 2 Immunostaining of A549 cells with anti-PDCD2, anti-γ–tubulin, anti-Ki-67, and DAPI. Cells were grown on coverslips for 72 hrs in media plus 0.1% FBS. (A, B) G1 arrested cells were directly fixed and stained. (C, D, E) Cells were stimulated with 10% FBS for 24 hrs then fixed and stained. **(A)** anti-PDCD2 plus anti-γ–tubulin. (B) anti-PDCD2 plus anti-Ki-67. (C) anti-PDCD2, (D) anti-PDCD2 plus anti-γ–tubulin. (E) anti-PDCD2 plus anti-Ki-67. Cells were counterstained with DAPI and examined with direct fluorescence.

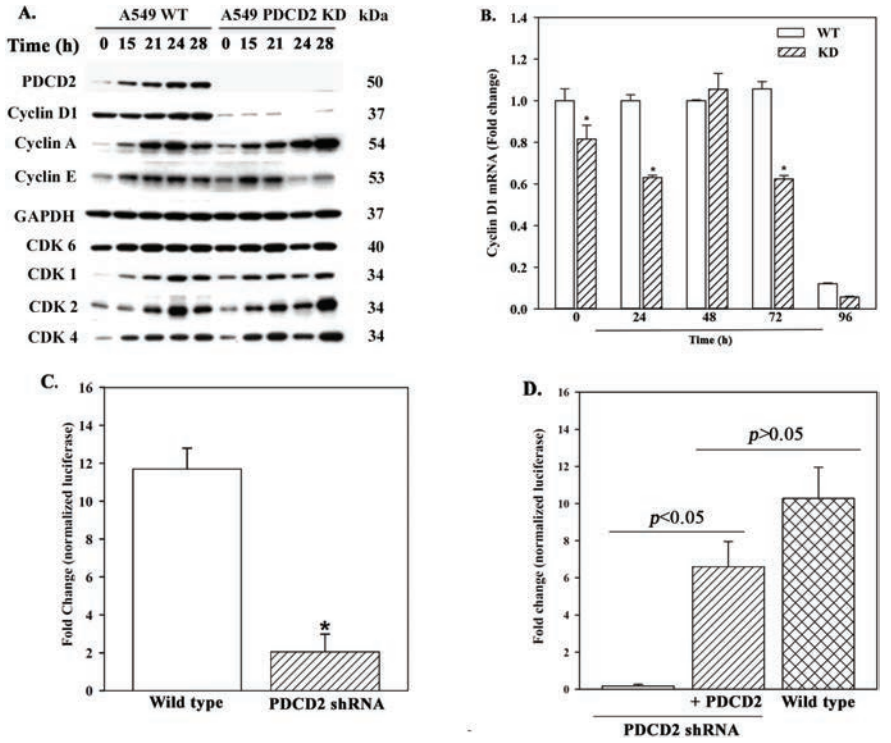

Figure 3 PDCD2 protein expression is associated with cell cycle progression in A549 cells. (A) Cells were cultured as in Figure 1. Crude lysates of total protein were loaded transferred and probed with PDCD2 and cell cycle-regulatory proteins. The proteins of interest were simultaneously exposed with GAPDH-HRP loading control. (B) Quantitative real time RT-PCR of Cyclin D1 RNA expression. (C, D) A549 WT, A549 PDCD2 KD cells, A549 empty vector and the resistant siRNA with PDCD2 expression (A549 PDCD2-KD+PDCD2 expression) were transfected with pCyclinD1-Luc and pβ-gal. The normalized values for the A549 WT cells with pGL3 alone were assigned a value of 1 and the experimental presented as the mean$\pm$SD fold changes.

cells up to 72 h (Figure 3B). The levels were decreased by 10 folds at 96 h, which coincided with the cells attaining confluence (Figure 3B).

The levels of cyclin D1 mRNA in the KD cells contrasted the levels noted in the WT cells. The levels were significantly ($p < 0.05$) decreased 0 and 24 h, as compared to WT cells. (Figure 3B). At 48 h, cyclin D1 mRNA levels were similar in the KD and WT cells. Beyond 48 h, there was a significant ($p < 0.05$) decrease in the KD cells (Figure 3B). These results indicated lowered cyclin D1 expression at 15 and 24 h in the PDCD2 KD, which is

consistent with the observed delay in PDCD2 KD cells entering cell cycle (Figure 1).

Decreased Reporter Gene Levels in PDCD2 KD Cells with the 5′ Regulatory Region of Cyclin D1

Since cyclin D1 mRNA levels were lowered after PDCD2 KD cells were induced into cycling (Figure 3B), we asked if this could be explained at the level of transcription. This question was addressed with a reporter gene system. Untransfected A549 cells (A549 WT), PDCD2 KD cells, A549 with empty vector (A549 EV), and PDCD2 KD cells reexpressed with PDCD2. All experimental cells were co-transfected with pCyclin D1-Luc and β-gal.

The normalized values for the A549 WT cells transfected with pGL3 alone were assigned values of 1 and the experimental points presented as the mean$\pm$SD fold changes. The results indicated significantly ($p < 0.05$) less luciferase with PDCD2 KD as compared to WT cells (Figure 3C). Rescue of PDCD2 in the KD cells led to a significant ($p < 0.05$) increase in luciferase as compareed to the KD cells (Figure 3D). However, the increase did not return to WT level (Figure 3D). Based on increased reporter gene activity when the cells were rescured with PDCD2, we concluded that cyclin D1 transcription partly required *PDCD2* expression.

Phospho (p)-Rb in A549-PDCD2 KD Cells

Since the retinoblastoma tumor suppressor protein (Rb) is required to release E2F for G1-S phase transition [29], we asked if delayed proliferation of PDCD2 KD cells can be explained by the inability of Rb to release E2F. Western blot showed minimal changes in Rb bands between the A459 WT and A549-PDCD2 KD cells (Figure 4). However, phospho-Rb, Ser780, Ser795, and Ser807/811 bands, which reflect endogenous levels of Rb phosphorylation at those specific sites, reached maximum expression at 15 to 21 h in A549 WT cells and then plateaued (Figure 4, Supplemental Figure 4). In contrast, the bands for phospho-Rb in the PDCD2 KD cells increased gradually, which correlated with delayed transition of cells to S phase (Supplemental Figure 4).

In A549 WT cells, E2F1 protein levels peaked at 15 h and remained highly consistent until the cells transited into the other phase of the cycle (28 h). In PDCD2 KD cells, E2F1 was undetectable at time 0 but peaked at 21 h, (6 h later than in A549-WT) and then decreased (Figure 4 and Supplemental Figure 4). These results strongly suggested that decreased

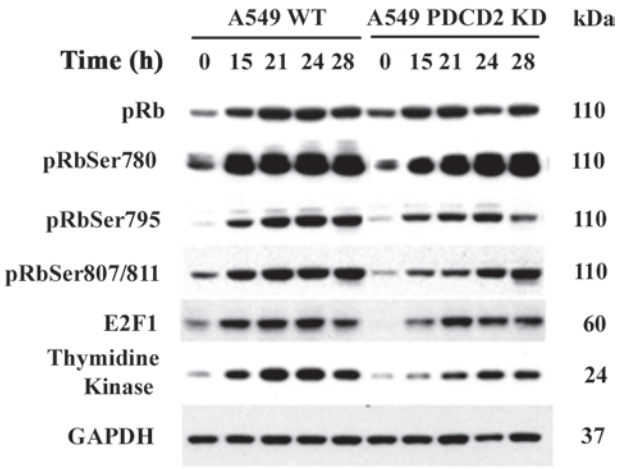

Figure 4 PDCD2 protein expression is associated with phosphorylated Rb in A549 cells. Cells were cultured as in Figure 1. Crude lysates of total protein were loaded transferred and probed with respective antibodies. The proteins of interest were simultaneously exposed with GAPDH-HRP loading control.

cyclin D1 in PDCD2 KD cells correlated with delayed phospho Rb. These findings would explain the delayed progression of the cell cycle in the PDCD2 KD cells. Taken together, these results identified the involvement of PDCD2 in regulating cell cycle relevant genes to influence cell proliferation.

Deregulation of the AKT/GSK3 Pathway in PDCD2 KD Cells

Glycogen synthase kinase 3β (GSK-3β) mediates nuclear export and cytoplasmic degradation of cyclin D1 protein [30, 31]. As a target of GSK-3β, cyclin D1 is induced by mitogenic stimulation. This induction is regulated by the Ras-phosphatidylinositol 3-kinase (PI3K)/AKT signaling pathway [27]. Our data showed a decrease of cyclin D1 in PDCD2 KD cells at the level of protein and transcription (Figure 2). We therefore asked if decreased cyclin D1 was GSK-3β-dependent. Immunoblots showed activation of GSK3β and AKT when we added FBS to A549 WT arrested cells. In contrast, despite serum activation of the A549 PDCD2 KD cells, GSK3β, which is normally dephosphorylated to degrade cyclin D1, remained downregulated (Figure 5A). These results indicated that decreased cyclin D1 in activated PDCD2 KD cells was independent of the GSK3β-PI3K/AKT pathway.

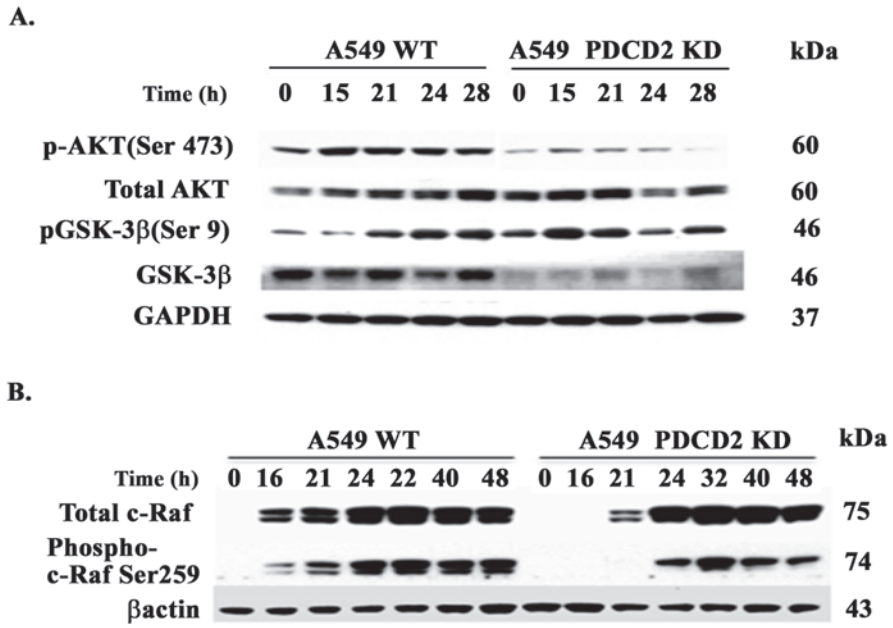

Figure 5 PI3K/AKT pathway associated with PDCD2 knockdown in A549 cells. G1 arrested A549-WT cells were stimulated with 10% FBS and harvested at different time points. (A) Western analysis of total AKT and GSK3B protein were compared to their activating phosphorylation state and probed with the respective antibody. (B) Expression of c-Raf and phospho c-Raf.

Ras/Raf/MEK/ERK and Ras/PI3K/Akt/mTOR Pathways in PDCD2 Expression

Compared to A549 WT cells, immunoblots with extracts from A549-PDCD2 KD cells, showed delay in Raf and p-Raf-Ser259 levels (Figure 5B). Since Cyclin D1 is a component of the mitogenic signaling pathway (Ras, PI3K/AKT pathway) [32], we asked if other mitogenic pathways were impacted by the absence of PDCD2. We also investigated if there were changes in the upstream stimuli that are involved with PDCD2 regulation. This led us to identify the signaling pathway involved in PDCD2 regulation. To address this question, we used A549 WT cells since these cells expressed PDCD2 (Figure 2). The cells were exposed to different pharmacological inhibitors at the time of induced cycling with media containing 10% FBS. We added vehicle (DMSO), Ly294002 (PI3K inhibitor), API-2 (AKT inhibitor), rapamycin (mTOR inhibitor) or U0126 (ERK inhibitor).

After 24 and 48 h, we analyzed PDCD2 levels by western blots with cell extracts. Compared to vehicle, at 24 h, inhibiting AKT and mTOR induced approximately 20% more PDCD2 (Figure 6A and Supplemental Figure 5). In contrast, inhibiting PI3K and ERK pathways caused 50% and 30% decreases of PDCD2, respectively (Figure 6A and Supplemental Figure 5). We noted similar changes at 48 h, albeit minimum increase when the PI3K pathway (AKT/ERK) was inhibited (Figure 6A). We deduced that PDCD2 may be associated with mitogen activated signaling. In contrast to PDCD2, these inhibitors did not alter cyclin D1 protein levels.

Specific Pathways in Cyclin D1 Reporter Gene Activity

Inhibiting PI3K led to decreased PDCD2 protein at 24 h without affecting cyclin D1 (Figure 6A). In order to dissect these pathways between PDCD2 and cyclin D1, we reverted to the reporter gene assay for cyclin D1 in A549 WT, which expresses PDCD2 protein. The transfectants included vehicle, or pharmacological inhibitors to NFκB or PKC. These inhibitors were selected because they could be second messenger molecules downstream of PI3K. In both cases, there were significant ($p < 0.05$) increases in luciferase activity as compared to vehicle, indicating that even in the presence of PDCD2 in the WT A549, cyclin D could be transcribed with suppressed activation of NFκB and PKC (Figure 6B). Similarly, PI3K inhibition significantly ($p < 0.05$) increased luciferase activity. Together, these results indicate that PDCD2 mediated increase in Cyclin D1 involves lowered mitogenic signaling molecules (PI3K, NFκB and PKC). Thus, although PDCD2 induced cell proliferation, the link between this molecule and mitogenic signaling molecules suggests a non-canonical pathway involving PDCD2.

PDCD2 Expression in Primary Human Lung Cancer

Using tissue arrays, we next investigated whether PDCD2 expression was increased in primary human lung cancer (Figure 7A). PDCD2 expression was predominately nuclear in the normal lung tissue controls. Analysis of tissue sections derived from six different lung cancer subtypes (squamous cell, small cell, large cell, adenocarcinoma, carcinoid and bronchioloalveolar carcinomas) revealed high PDCD2 expression in most cases. While PDCD2 expression was predominately nuclear in normal lung tissues, a significant degree of cytoplasmic staining was apparent in cancer tissues. The differences in PDCD2 subcellular localization between normal controls and lung cancer samples proved to be highly statistically significant (Figure 7B).

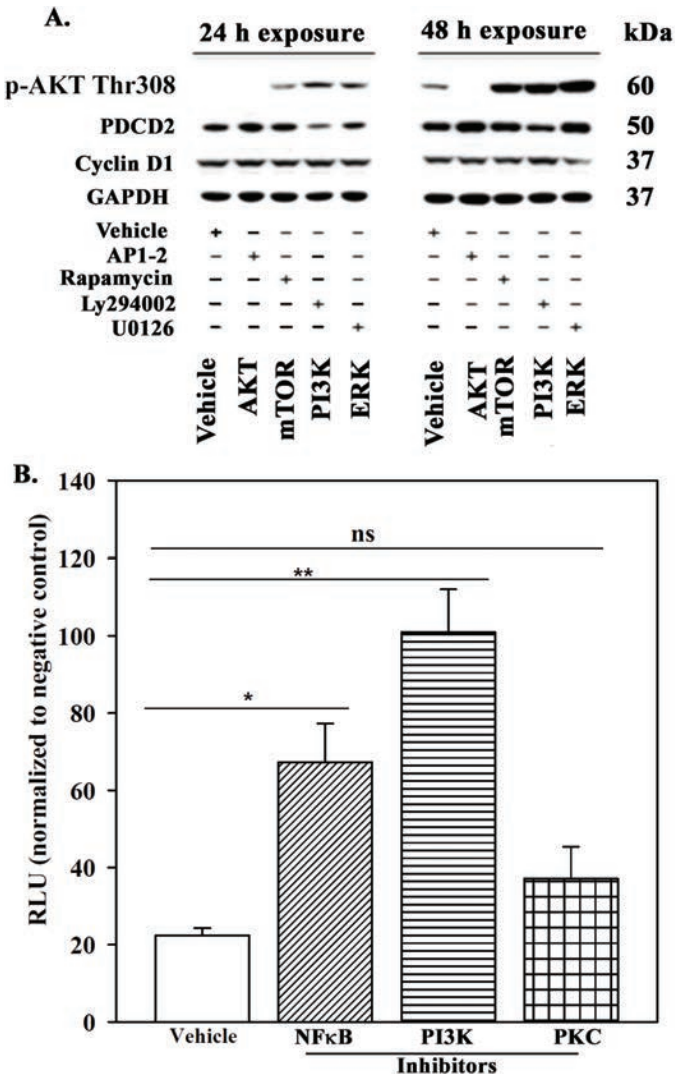

Figure 6 Analysis of the upstream signaling pathway for the regulation of PDCD2 expression. (A) 0.7×10^6 A549 WT cells were synchronized by serum starvation in media with 0.1% FBS. After 72 hrs, the cells were stimulated with media plus 10% FBS and then treated with vehicle, 1 μM API-2, 100 nM rapamycin, 35 μM Ly294002, and 20 μM U0126. (B) A549 WT cells were transfected with pCyclinD1-Luc and pβ-gal. Transfectants were treated with the stated inhibitors. The normalized luciferase activity is presented as fold change over transfectants with pGL3 alone. The mean$\pm$SD fold change represent four independent experiments.

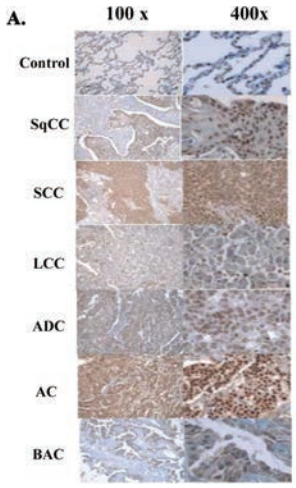

B.

Tissue type	No Stain	Nuc	Cyto	Nuc + Cyto	Total	*p*-value
Normal Lung Tissue	0	19	0	1	20	Normal/ Cancer
Squamous Cell Carcinoma	8	9	4	24	45	0.000001
Small Cell Carcinoma	2	4	0	10	16	0.0001
Large Cell Carcinoma	4	2	0	1	7	0.0005
Adenocarcinoma	15	2	20	20	57	0.000001
Atypical carcinoid	0	2	0	8	10	0.0001
Bronchioloalveolar carcinoma	0	0	8	0	8	0.000001

Figure 7 PDCD2 expression in lung cancer. Tissue arrays including normal lung tissue and sections from several subtypes of Lung cancer were analyzed by immunohistochemistry for PDCD2 protein expression. (C) Normal lung, (SqCC) squamous cell carcinoma, (SCC) small cell carcinoma, (LCC) large cell carcinoma, (ADC) adenocarcinoma, (AC) carcinoid, (BAC) bronchioloalveolar carcinoma. Magnification 100X and 400X as indicated. The amount of PDCD2 staining was evaluated by a pathologist and the differences in PDCD2 subcellular localization between normal controls and lung cancer samples proved to be highly statistically significant.

Discussion

We previously reported that stable knockdown of PDCD2 in A549 cells resulted in slower proliferation compared to parental A549 WT cells [21]. This study analyzed the cell cycle delay to G1/S transition when PDCD2 was KD in A549 cells (Figure 1). Wild-type quiescent cells showed PDCD2 localized in the plasma membrane and nucleus (Figure 2). Serum stimulation led to ubiquitous PDCD2 expression in the cells (Figure 2). We found that the delay in G1/S transition correlated to low expression of cyclin D1. However, in cause effect studies, when we reexpressed PDCD2, cyclin D1 level was increased (Figure 3). Additionally, we observed dysregulation of cell cycle-associated proteins and components of the PI3K/Akt and MAPK/Erk in the PDCD2 KD cells (Figures 3–5). A549 wild type cells, when exposed to inhibitors of the PI3K/Akt and MAPK/Erk pathways, resulted in decreased PDCD2 (Figure 6). Herein, these observations suggest that PDCD2 is involved in cell cycle progression and proliferation via a mitogen activated pathway.

Immunostaining of quiescent A549 WT cells showed that unlike the prototypical markers for DNA synthesis, Ki67 and γ–tubulin which localized either in the nuclei or cytoplasm respectively with, PDCD2, which localizes in both the nuclei and the plasma membrane (Figure 2). This expression could potentially be the result of the presence of two spliced variants that encode different PDCD2 proteins, a 228 aa and a 344 aa with the longer isoform containing a conserved tyrosine domain [33]. Opposite from quiescent cells, in proliferating A549-WT cells, immunostaining shows ubiquitous PDCD2 expression (Figure 2), which increases even more during cytokinesis (Figure 2). Hence, we suggest that PDCD2 is involved in the regulation of cell proliferation. These results are supported by our analysis of tissue sections derived from six different lung cancer subtypes. In this analysis PDCD2 expression was predominately nuclear in normal lung tissues, with a significant degree of cytoplasmic staining apparent in cancer tissues (Figure 7).

Cyclin D1 is a component of the mitogenic signaling pathway (Ras, PI3K/AKT pathway), its nuclear export and cytoplasmic degradation may be mediated by or independent [32, 34, 35] of GSK3β phosphorylation. Our results indicate that regulation of cyclin D1 in A549 cells may be independent of GSK3 phosphorylation (Figure 5). Thus, we suggest that the decrease in expression of cyclin D1 in the PDCD2 KD cells is not a product of degradation but of transcriptional dysregulation. An extranuclear function of cyclin D1 is to enhance proliferation by phosphorylating Akt1 at Ser473 [36]. The low expression of p-Akt (Ser473) observed in the PDCD2 knockdown cells coincided with the low expression of cyclin D1 (Figures 5). Therefore, the decrease of cyclin D1 in the PDCD2 KD cells is reflected in the decrease in activity of p-AKT (Ser 473), and cell proliferation (Figures 1 and 5). These results support the notion that slow proliferation in PDCD2 KD cells maybe a result of decreases in cyclin D1 and AKT.

Cyclin D1 phosphorylates pRb, promotes G1/S transition, releases the activating E2Fs, and the transcription of genes required for DNA synthesis [37]. Phospho (p) Rb and E2F1 proteins are expressed differently in A549 WT and PDCD2 knockdown cells (Figure 4). Precise dynamics of E2F are necessary for the proper timing of cell cycle entry, and precocious, prolonged, elevated, or reduced accumulation of E2F results in replication stress culminating in either cell arrest or death [39]. Consequently, the different expression patterns may implicate that the E2F family maybe the source for the delayed G1/S transition in the PDCD2 knockdown cells.

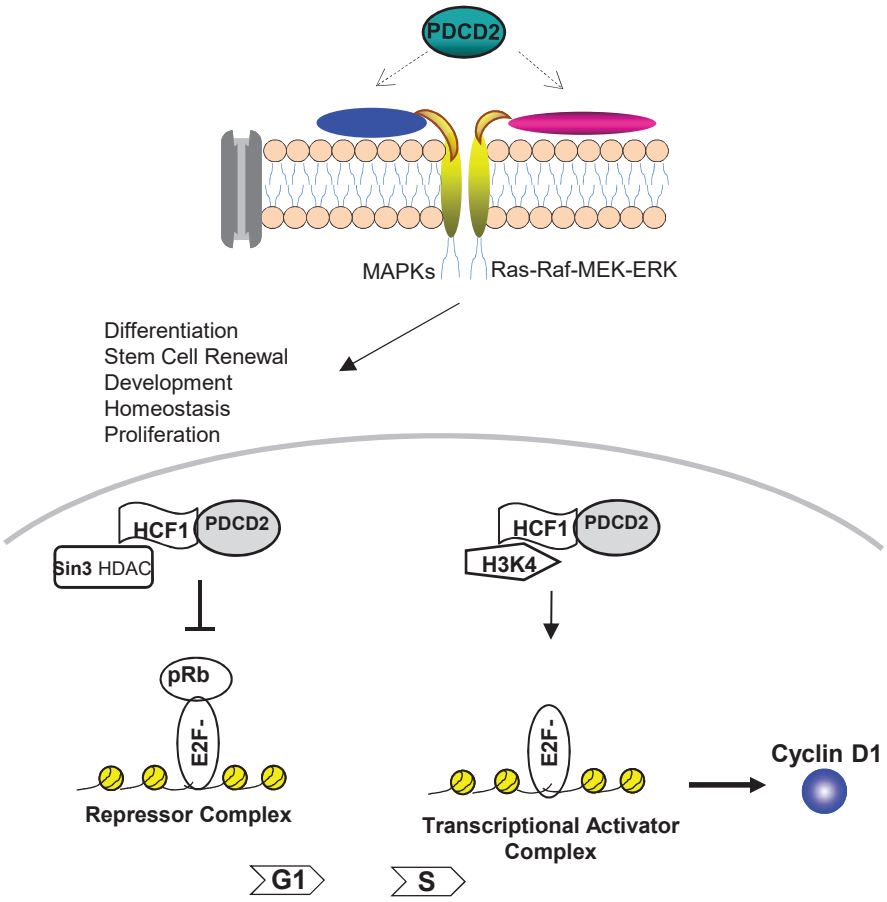

Figure 8 Model for the propose PDCD2 mode of action. The plasma membrane PDCD2 interacts with MAPKs to influence processes such as differentiation and proliferation. At the nuclear level via its association to the C-terminus of the host cell factor (Scarr et al. 2002), PDCD2 is part of the "E2F-1 repressor complex" (Tyagi et al. 2007) and of the transcriptional activator complex, "HCF-1/H3K4/E2F1" for specific transcription of genes involved in the G1/S transition.

Cyclin D1 can be regulated transcriptionally and post-translationally [38, 39]. Its promoter region contains multiple binding sites for transcription factors to regulate proliferation, differentiation, development, tissue specificity, specialized stimulation and inhibition (Reviewed in [39]). These multiple transcription factors could not override the downregulation of cyclin D1

observed in the PDCD2 knockdown cells. In assays using human luciferase-promoter constructs, E2F-1 overexpression can repress cyclin D1 protein levels; full repression requires E2F's DNA binding domain, its pRb binding domain, and its Sp1 binding domain [40]. The precise mechanism leading to regulation of cyclin D1 by PDCD2 remains unclear and in this study, we are proposing a model where PDCD2 at the nuclear level could potentially regulate cyclin D1 through an association with the E2F family of transcription factors (Figure 8). The PDCD2 MYND-type domain associates to the C-terminus of the host cell factor 1 (HCF-1_c) [15], a multidomain protein [41] that modulates different phases of the cell cycle. HCF-1_c-PDCD2 has been suggested to have an associated suppressive activity on the transcription of genes required to drive the cell cycle [15]. HCF-1 activates transcription by recruiting H3K4 to E2F1 responsive promoters [18, 42]. At the G1/S transition after sequential CDK phosphorylation, the HCF-1/H3K4/E2F1 complex deactivates the G1 repressor complex formed by pRb, E2F1 and Sin3 HDAC leading to transcriptional activation [18]. Hypothetically, in our model we propose, PDCD2 is part of the HCF-1/H3K4/E2F1 transcriptional activator complex. In the absence of PDCD2, there is downregulation of cyclin D1, untimely activation of genes responsible for the G1/S transition, and delayed cell cycle progression resulting in slow proliferation.

Based on the delayed expression and activation of c-Raf, decreased activation of p-Akt (Ser473), and the decreased expression of PDCD2 when wild-type cells are exposed to Akt and Erk inhibitors, we suggest that the PDCD2 isoform localized on the plasma membrane mediates activation of mitogen receptors that affect Akt and Erk signaling (Figure 8). At the plasma membrane level, we suggest PDCD2 regulates functions such as differentiation, stem cell renewal, development, homeostasis, and proliferation [5, 10–13, 21].

The fact that the low expression of cyclin D1 observed in PDCD2 KD cells, and corroboration with cyclin D1 promoter activity, further support the notion that PDCD2 maybe transcriptionally regulating cyclin D1. Deregulation of cyclin D1 is often associated with human malignancies. Therefore, these findings may have implications in the development of clinical applications.

Acknowledgements

The authors thank Dr. Joseph Bertino for his invaluable advice and design of the experiments throughout the research process.

References

[1] G.P. Owens, W.E. Hahn, J.J. Cohen, Identification of mRNAs associated with programmed cell death in immature thymocytes, Mol Cell Biol, 11 (1991) 4177–4188.

[2] B.W. Baron, E. Hyjek, B. Gladstone, M.J. Thirman, J.M. Baron, PDCD2, a protein whose expression is repressed by BCL6, induces apoptosis in human cells by activation of the caspase cascade, Blood Cells Mol Dis, 45 (2002) 169–175.

[3] B.W. Baron, J. Anastasi, M.J. Thirman, Y. Furukawa, S. Fears, D.C. Kim, F. Simone, M. Birkenbach, A. Montag, A. Sadhu, The human programmed cell death-2 (PDCD2) gene is a target of BCL6 repression: implications for a role of BCL6 in the down-regulation of apoptosis, Proceedings of the National Academy of Sciences, 99 (2002) 2860–2865.

[4] Q. Chen, K. Qian, C. Yan, Cloning of cDNAs with PDCD2 C domain and their expressions during apoptosis of HEK293T cells, Molecular and cellular biochemistry, 280 (2005) 185–191.

[5] S. Minakhina, M. Druzhinina, R. Steward, Zfrp8, the Drosophila ortholog of PDCD2, functions in lymph gland development and controls cell proliferation, Development, 134 (2007) 2387–2396.

[6] I. Guénal, B. Mignotte, Studies of specific gene induction during apoptosis of cell lines conditionally immortalized by SV40, FEBS letters, 374 (1995) 384–386.

[7] D.L. Vaux, G. Hacker, Cloning of mouse RP-8 cDNA and its expression during apoptosis of lymphoid and myeloid cells, DNA and cell biology, 14 (1995) 189–193.

[8] B.W. Baron, N. Zeleznik-Le, M.J. Baron, C. Theisler, D. Huo, M.D. Krasowski, M.J. Thirman, R.M. Baron, J.M. Baron, Repression of the PDCD2 gene by BCL6 and the implications for the pathogenesis of human B and T cell lymphomas, Proceedings of the National Academy of Sciences, 104 (2007) 7449–7454.

[9] D. Steinemann, S. Gesk, Y. Zhang, L. Harder, C. Pilarsky, B. Hinzmann, J.I. Martin-Subero, M.J. Calasanz, A. Mungall, A. Rosenthal, Identification of candidate tumor-suppressor genes in 6q27 by combined deletion mapping and electronic expression profiling in lymphoid neoplasms, Genes, Chromosomes and Cancer, 37 (2003) 421–426.

[10] W. Mu, R.J. Munroe, A.K. Barker, J.C. Schimenti, PDCD2 is essential for inner cell mass development and embryonic stem cell maintenance, Developmental biology, 347 (2010) 279–288.
[11] J. Kramer, C.J. Granier, S. Davis, K. Piso, J. Hand, A.B. Rabson, H.E. Sabaawy, PDCD2 controls hematopoietic stem cell differentiation during development, Stem Cells Dev, 22 (2013) 58–72.
[12] S. Minakhina, R. Steward, Hematopoietic stem cells in Drosophila, Development, 137 (2010) 27–31.
[13] N.A. Kokorina, C.J. Granier, S.O. Zakharkin, S. Davis, A.B. Rabson, H.E. Sabaawy, PDCD2 knockdown inhibits erythroid but not megakaryocytic lineage differentiation of human hematopoietic stem/progenitor cells, Experimental hematology, 40 (2012) 1028–1042. e1023.
[14] C.J. Granier, W. Wang, T. Tsang, R. Steward, H.E. Sabaawy, M. Bhaumik, A.B. Rabson, Conditional inactivation of PDCD2 induces p53 activation and cell cycle arrest, Biology open, 3 (2014) 821–831.
[15] R.B. Scarr, P.A. Sharp, PDCD2 is a negative regulator of HCF-1 (C1), Oncogene, 21 (2002) 5245–5254.
[16] H. Goto, S. Motomura, A.C. Wilson, R.N. Freiman, Y. Nakabeppu, K. Fukushima, M. Fujishima, W. Herr, T. Nishimoto, A single-point mutation in HCF causes temperature-sensitive cell-cycle arrest and disrupts VP16 function, Genes and Development, 11 (1997) 726–737.
[17] J. Wysocka, W. Herr, The herpes simplex virus VP16-induced complex: the makings of a regulatory switch, Trends in biochemical sciences, 28 (2003) 294–304.
[18] S. Tyagi, A.L. Chabes, J. Wysocka, W. Herr, E2F activation of S phase promoters via association with HCF-1 and the MLL family of histone H3K4 methyltransferases, Molecular cell, 27 (2007) 107–119.
[19] T. Heinzel, R.M. Lavinsky, T.-M. Mullen, M. Söderström, C.D. Laherty, J. Torchia, W.-M. Yang, G. Brard, S.D. Ngo, J.R. Davie, A complex containing N-CoR, mSln3 and histone deacetylase mediates transcriptional repression, Nature, 387 (1997) 43–48.
[20] B. Lutterbach, D. Sun, J. Schuetz, S.W. Hiebert, The MYND motif is required for repression of basal transcription from the multidrug resistance 1 promoter by the t (8; 21) fusion protein, Molecular and cellular biology, 18 (1998) 3604–3611.
[21] N. Barboza, S. Minakhina, D.J. Medina, B. Balsara, S. Greenwood, L. Huzzy, A.B. Rabson, R. Steward, D.G. Schaar, PDCD2 functions in cancer cell proliferation and predicts relapsed leukemia, Cancer biology & therapy, 14 (2013) 546–555.

[22] J. Qian, G. Yehia, C.A. Molina, A. Fernandes, R.J. Donnelly, D.J. Anjaria, P. Gascon, P. Rameshwar, Cloning of human preprotachykinin-I promoter and the role of cyclic adenosine 5'-monophosphate response elements in its expression by IL-1 and stem cell factor, The Journal of Immunology, 166 (2001) 2553–2561.

[23] S.A. Patel, S.H. Ramkissoon, M. Bryan, L.F. Pliner, G. Dontu, P.S. Patel, S. Amiri, S.R. Pine, P. Rameshwar, Delineation of breast cancer cell hierarchy identifies the subset responsible for dormancy, Scientific reports, 2 (2012) 906.

[24] J. Debnath, S.K. Muthuswamy, J.S. Brugge, Morphogenesis and oncogenesis of MCF-10A mammary epithelial acini grown in three-dimensional basement membrane cultures, Methods, 30 (2003) 256–268.

[25] T.G. Graves, M.W. Harr, E.L. Crawford, J.C. Willey, Stable low-level expression of p21WAF1/CIP1 in A549 human bronchogenic carcinoma cell line-derived clones down-regulates E2F1 mRNA and restores cell proliferation control, Molecular cancer, 5 (2006) 1–13.

[26] R.N. Gunawardane, S.B. Lizarraga, C. Wiese, A. Wilde, Y. Zheng, γ-Tubulin complexes and their role in microtubule nucleation, Current topics in developmental biology, 49 (1999) 55–73.

[27] B. Raynaud-Messina, A. Merdes, γ-tubulin complexes and microtubule organization, Current opinion in cell biology, 19 (2007) 24–30.

[28] X. Sun, P.D. Kaufman, Ki-67: more than a proliferation marker, Chromosoma, 127 (2018) 175–186.

[29] F.A. Dick, S.M. Rubin, Molecular mechanisms underlying RB protein function, Nature reviews Molecular cell biology, 14 (2013) 297–306.

[30] J.A. Diehl, M. Cheng, M.F. Roussel, C.J. Sherr, Glycogen synthase kinase-3β regulates cyclin D1 proteolysis and subcellular localization, Genes & development, 12 (1998) 3499–3511.

[31] J.A. Diehl, F. Zindy, C.J. Sherr, Inhibition of cyclin D1 phosphorylation on threonine-286 prevents its rapid degradation via the ubiquitin-proteasome pathway, Genes & development, 11 (1997) 957–972.

[32] L. Jirmanova, M. Afanassieff, S. Gobert-Gosse, S. Markossian, P. Savatier, Differential contributions of ERK and PI3-kinase to the regulation of cyclin D1 expression and to the control of the G1/S transition in mouse embryonic stem cells, Oncogene, 21 (2002) 5515–5528.

[33] T. Kawakami, Y. Furukawa, K. Sudo, H. Saito, S. Takami, E. Takahashi, Y. Nakamura, Isolation and mapping of a human gene (PDCD2) that is

highly homologous to Rp8, a rat gene associated with programmed cell death, Cytogenetic and Genome Research, 71 (1995) 41–43.

[34] J.R. Alt, J.L. Cleveland, M. Hannink, J.A. Diehl, Phosphorylation-dependent regulation of cyclin D1 nuclear export and cyclin D1–dependent cellular transformation, Genes & development, 14 (2000) 3102–3114.

[35] D. Germain, A. Russell, A. Thompson, J. Hendley, Ubiquitination of free cyclin D1 is independent of phosphorylation on threonine 286, Journal of Biological Chemistry, 275 (2000) 12074–12079.

[36] K. Chen, X. Jiao, A. Di Rocco, D. Shen, S. Xu, A. Ertel, Z. Yu, G. Di Sante, M. Wang, Z. Li, Endogenous cyclin D1 promotes the rate of onset and magnitude of mitogenic signaling via Akt1 Ser473 phosphorylation, Cell reports, 32 (2020).

[37] T. Sladek, E2F transcription factor action, regulation and possible role in human cancer, Cell proliferation, 30 (1997) 97–105.

[38] J. Langenfeld, H. Kiyokawa, D. Sekula, J. Boyle, E. Dmitrovsky, Post-translational regulation of cyclin D1 by retinoic acid: a chemoprevention mechanism, Proceedings of the National Academy of Sciences, 94 (1997) 12070–12074.

[39] J.P. Alao, The regulation of cyclin D1 degradation: roles in cancer development and the potential for therapeutic invention, Molecular cancer, 6 (2007) 1–16.

[40] G. Watanabe, C. Albanese, R.J. Lee, A. Reutens, G. Vairo, B. Henglein, R.G. Pestell, Inhibition of cyclin D1 kinase activity is associated with E2F-mediated inhibition of cyclin D1 promoter activity through E2F and Sp1, Molecular and cellular biology, 18 (1998) 3212–3222.

[41] A.C. Wilson, M. Boutros, K.M. Johnson, W. Herr, HCF-1 amino-and carboxy-terminal subunit association through two separate sets of interaction modules: involvement of fibronectin type 3 repeats, Molecular and Cellular Biology, 20 (2000) 6721–6730.

[42] E. Julien, W. Herr, A switch in mitotic histone H4 lysine 20 methylation status is linked to M phase defects upon loss of HCF-1, Molecular cell, 14 (2004) 713–725.